PROCEEDINGS, Twelfth Workshop on Geothermal Reservoir Engineering
Stanford University, Stanford, California, January 20-22, 1987
SGP-TR-109

Interference Tests at Kawerau, New Zealand*

John G. Burnell and Mark J. McGuinness

Applied Mathematics Division, DSIR
Wellington, NewZealand

Abstract

Analysis of interference tests at the Kawerau geothermal field in New Zealand has indicated that the reservoir may be viewed on a coarse scale as a two-layer structure. While these layers have high permeabilities, they are in poor hydrological communication with each other. The shallower layer is modelled as a finite cylindrical reservoir. The deeper layer is modelled as a larger cylindrical reservoir with recharge from the sides. The fitted permeabilities and storativities suggest the importance of flow in fractures at Kawerau.

1 Introduction

The Kawerau geothermal field has been in production since 1956, and supplies steam at up to 270 t/hr to the Tasman Pulp and Paper mill. The early shallow wells ceased production within four years, due to cooling of the production zone, and the steam supply was maintained by drilling deeper. The deeper wells have lasted longer, and cooling has led to progressively deeper wells and more exploratory wells.

During August, September and October 1985, interference testing was carried out at Kawerau by the Ministry of Works and Development, Wairakei. Seven wells were monitored (Figure 1), KaM1, KaM2, KaM4, Ka11, Ka14, Ka17 and Ka31. KaM3 was used as an injection well. The two major producing wells at the time, Ka21 and Ka35, were throttled back (see Figures 2, 3 and 4). Responses fell into two groups, with the shallower feeding wells responding to injection into the shallow feeding KaM3, and the deeper feeding wells responding to the changes in production of the deep feeding Ka21 and Ka35. Ka14, which feeds at intermediate depth, responds only to Ka21, suggestive of more complicated structure.

	KaM1	KaM2	KaM4	Ka11
kh (d-m)	575	392	511	1600
ϕch (m/Pa $\times 10^{-7}$)	2.6	6.9	1.6	3.5
ϕcV (m^3/Pa)	16	18	26	10

Table 1: Parameter values obtained from fitting a finite reservoir model to the shallow responses to KaM3. A dynamic viscosity for 150°C water of $\mu = 1.8 \times 10^{-4}$ Pa.s was assumed.

2 Shallow Responses

The wells with responses to injection into KaM3 had varying transient pressure changes, and also featured net pressure increases of 2 to 4 KPa. These pressure increases would be consistent with a finite reservoir effect. Hence the shallow reservoir was modelled as a cylinder with no-flow boundaries. The solution in Matthews and Russell (p.11) was simplified into three parts, an early time transient line-source exponential integral solution, a late time steady drawdown solution, and a linear intermediate time segment joining the other two parts (Burnell and McGuinness, 1986). This finite cylindrical reservoir solution, together with atmospheric pressure variations, was fitted to each responding well numerically, using standard nonlinear least-squares routines from the NAG library on the Applied Mathematics Division VAX. The fits obtained are plotted in Figures 5, 6, 7 and 8. The fitted parameter values obtained are in Table 1.

2.1 Results

If the storativity ϕch in Table 1 is interpreted for a model of the shallow reservoir as a closed box of fluid, with a compressibility $c = 4 \times 10^{-10}$ Pa^{-1} for 150°C water, and using the depth $h = 500$ m, unrealistically large values of porosity ϕ of 0.78–3.5 result. If the reservoir is modelled as open-topped, with an effective compressibility $c = 1/\rho gh = 2 \times 10^{-7}$ Pa^{-1}, the porosity ϕ takes values ranging from about 0.001 to

*this analysis was made under contract to the Gas and Geothermal Trading Group, Ministry of Energy, Wellington, New Zealand

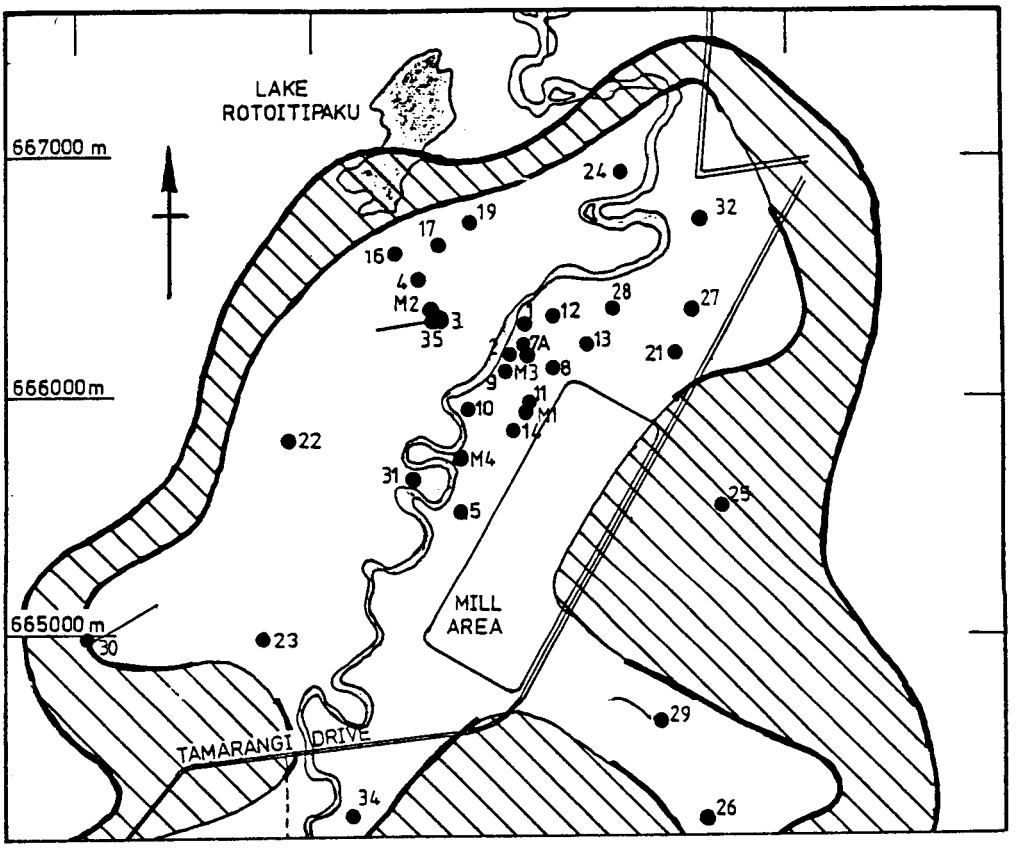

Feed Depths of the Bores (metres), with the major feed listed first.

KAM1	145
KAM2	130, 95, 112
KAM3	100
KAM4	85
KA11	400
KA14	800, 500
KA17	930, 1360
KA21	1080, 710, 800, 1160
KA31	1500, 700, 1100
KA35	1010

Figure 1: Wellsites at the Kawerau Geothermal Field and Feed Depths.

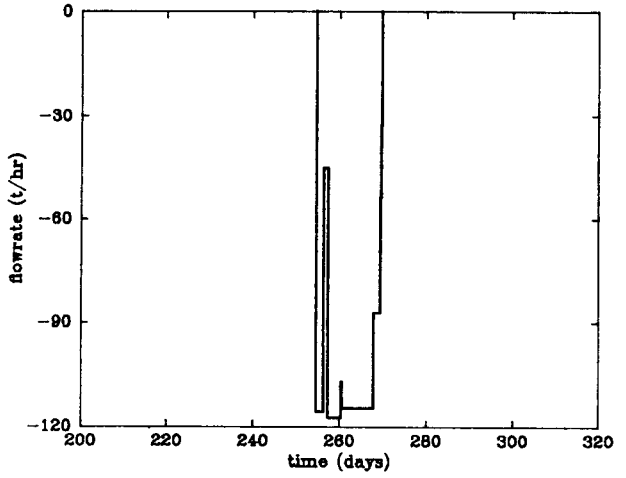

Figure 2: Measured Flowrate Changes in KaM3

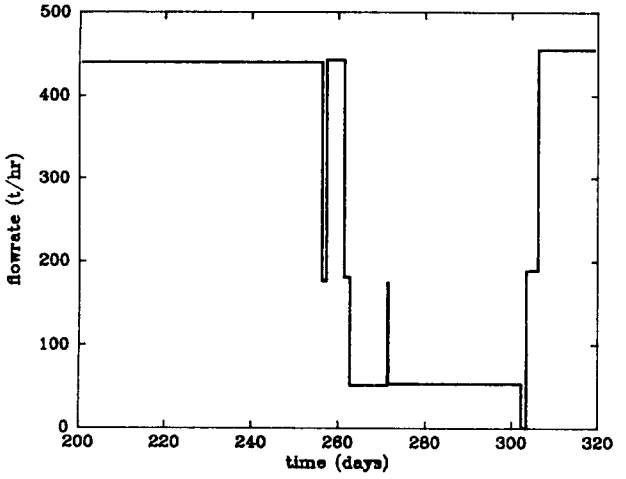

Figure 3: Measured Flowrate Changes in Ka21.

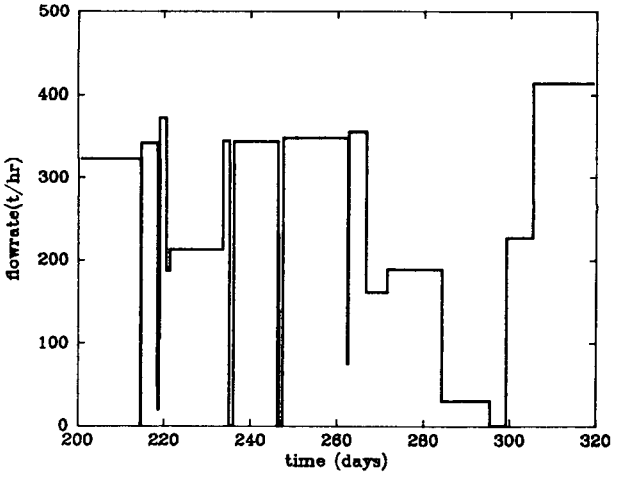

Figure 4: Measured Flowrate Changes in Ka35.

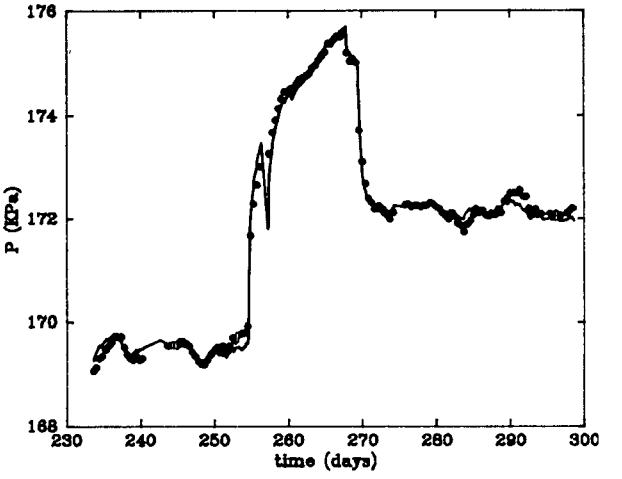

Figure 5: KaM1 pressure data and fitted finite reservoir response to KaM3.

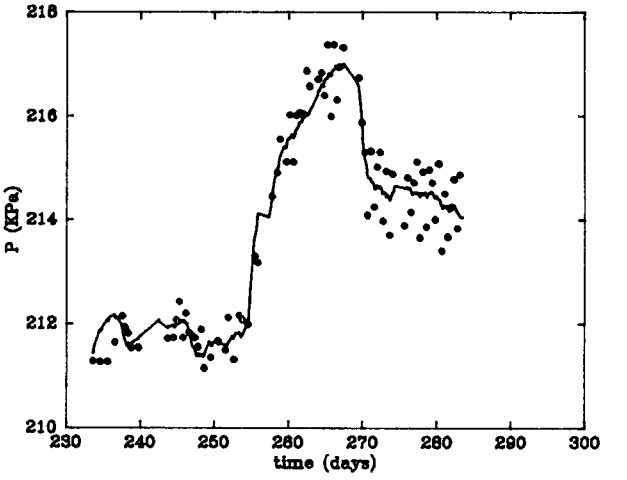

Figure 6: KaM2 pressure data and fitted finite reservoir response to KaM3.

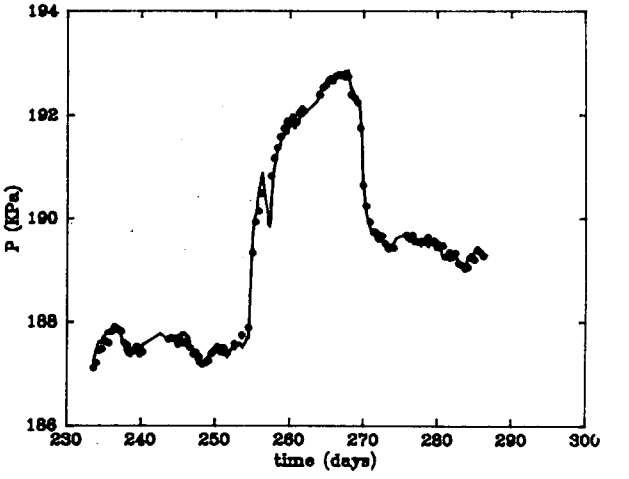

Figure 7: KaM4 pressure data and fitted finite reservoir response to KaM3.

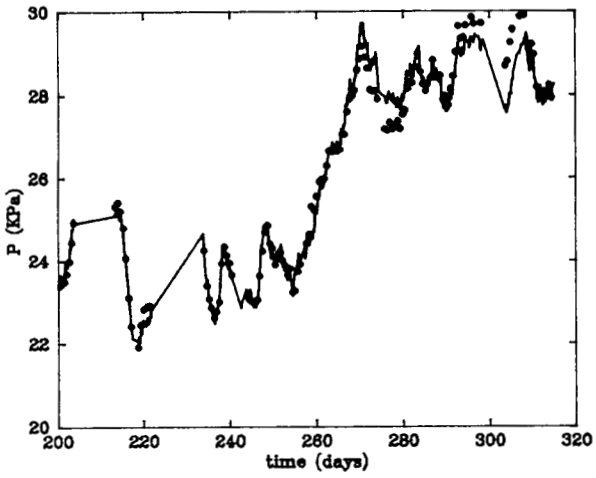

Figure 8: Ka11 pressure data and fitted finite reservoir response to KaM3.

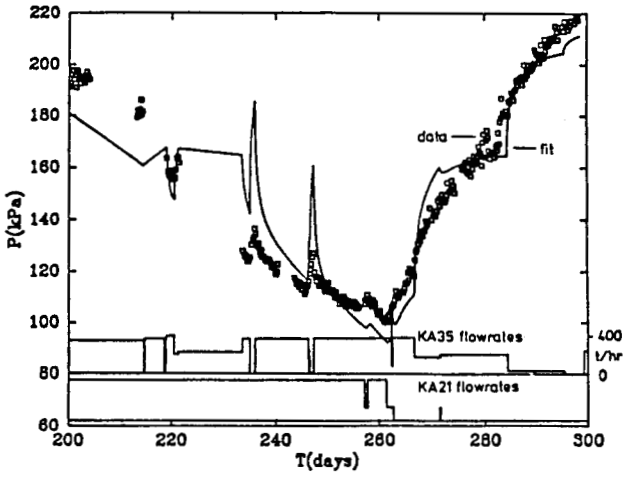

Figure 9: Ka17 pressure data and fitted Theis solution response to Ka21 and Ka35.

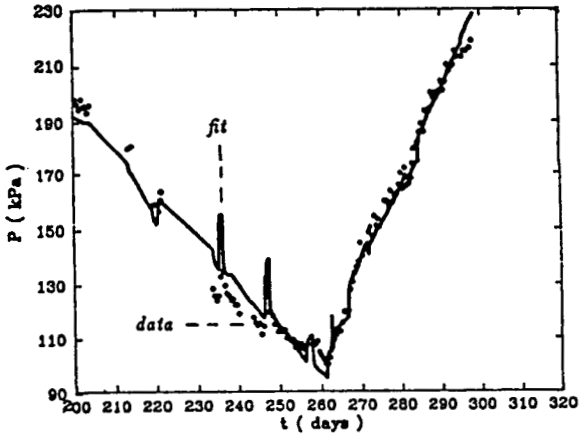

Figure 10: Ka17 pressure data and fitted finite reservoir with recharge response to Ka21 and Ka35. Uniform permeabilities were used.

0.007. This porosity is very small, suggesting a fracture network, at least at the fluid surface.

The values fitted to kh and ϕch are obtained from the early-time transient part of the model solution. The value of the storage coefficient ϕcV is obtained from fitting the late-time part of the model solution. If the early-time values of ϕch are used together with $h = 500$ m, a shallow reservoir volume in the range 14–87 Km^3 is obtained, or an area in the range 28–164 Km^2. This is much larger than expected at Kawerau — the area inside the resistivity boundary is 6–10 Km^2. This implies that the shallow reservoir may be in good hydrological communication with surrounding cooler groundwaters. An alternative possibility is that the early-time values of ϕch might not be appropriate at later times, due to double-porosity behaviour. Under this option, the early-time storativity is dominated by high permeability, low porosity fractures or contacts between layers of different reservoir materials, while at later times a higher storativity is obtained as the effect of blocks or layers of lower permeability material becomes important (see, for example, Gringarten, 1984, Moench, 1984 and McGuinness, 1986). Assuming the late-time storativity corresponds to a porosity $\phi = 0.2$, a compressibility $c = 2 \times 10^{-7}$ Pa^{-1} and a depth $h = 500$ m gives a reservoir surface area in the range 0.5–1.3 Km^2.

3 Deep Responses

The deeper-feeding wells Ka17 and Ka31 responded to changes in production of Ka21 and Ka35. Ka14, which has a major feed at intermediate depth, responds only to Ka21 within measurement accuracy.

Recharge is expected to be important in modelling the deeper responses, since the deeper reservoir has been under production for many years, and reservoir pressures have not dropped more than 2 bars (Grant, 1985). Hence a cylindrical reservoir with pressure-dependent recharge from the sides was chosen as a model. This model is developed and solved for in Burnell and McGuinness, 1986. The solution is simplified in a similar approach to that used for the shallow model, with an early-time transient solution merging into a late-time steady-state solution.

For comparison purposes, the response at Ka17 was initially fitted with the infinite-acting exponential integral solution. The effects of flowrate changes in Ka21 and Ka35 were superposed. The numerical pro-

	Ka17	Ka31	Ka14
$k_{35}h$ (d-m)	585	679	
$k_{21}h$ (d-m)	48	95	390
ϕch (m/pa$\times 10^{-7}$)	1.1	0.9	12.0
ϕcV (m^3/pa)	35	41	34
γ (m^3/Pa.s$\times 10^{-6}$)	.25	1.5	7.0

Table 2: Parameter values from fitting the cylindrical reservoir with recharge to deep responses. A dynamic viscosity for 270°C water of $\mu = 1.0 \times 10^{-4}$ Pa.s was assumed.

cedure converged to the fit shown in Figure 9. The response to long-term production was simply modelled as a linear trend. This fit is used as a reference with which improvements may be compared.

An improved fit is obtained when the model developed in Burnell and McGuinness (1986) is used. Figure 10 shows the resulting fit. The short-time pulse-like responses to changes in Ka35 flowrates are not very accurately modelled. With the possibility of vertical structure in mind, the permeability used in responses to Ka21 was allowed to be different to the permeability used in responses to Ka35. This further improved the fit, as seen in Figure 11. This model, of a cylinder with lateral recharge and different permeabilities for Ka21 and Ka35, was also successfully fitted to the responses of Ka31 and Ka14 (see Figures 12 and 13). The response of Ka14 to Ka35 flowrate changes was not significantly different from zero. The parameter values obtained from these fits are presented in Table 2.

Other wells in production at the time of the test constituted about 20% of the maximum total mass flowrate. While these wells, Ka16, Ka19, Ka27 and Ka28 were not continuously monitored, records of when they were shut and what their average flowrate was, were incorporated into the model. Ka16, which went on bleed near the beginning of the test, has been found to be in poor communication with Ka17 (McGuinness, 1985), and was ignored. The small changes (up to 50 t/hr) in the flowrate of Ka28 were incorporated into the Ka21 flowrate changes. Ka21 and Ka27 discharge into the same separator and are treated as one well since their flowrates are measured as a combined one. The flowrate changes in Ka19 were added into those for Ka35, since Ka35 took over from Ka19 on day 213. Startup time for Ka19 (Ka35) was taken from a workover which improved production at about day 0. Startup time for Ka21 was also taken to be day 0. This was an arbitrary choice, and subsequent information indicates that a better choice would be about five years earlier. These factors reduce the reliability of the results, especially the estimates of recharge and field size. In general, changing to an earlier startup time for Ka21 would be expected to increase the estimated field size and the estimated recharge to the field, making these results conservative.

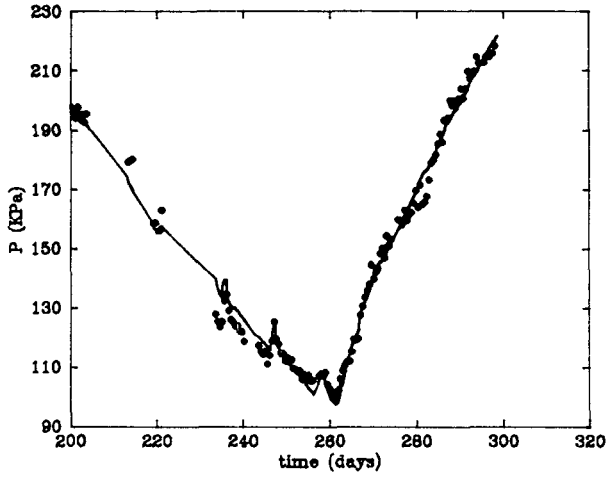

Figure 11: Ka17 pressure data and fitted finite reservoir with recharge response to Ka21 and Ka35. Permeabilities were allowed to differ for the two source wells.

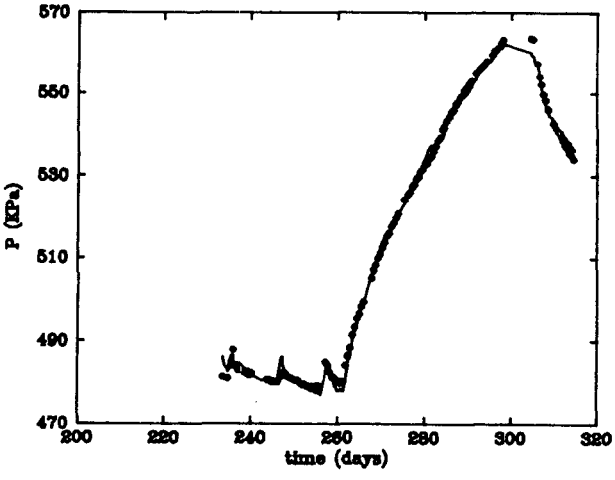

Figure 12: Ka31 pressure data and fitted finite reservoir with recharge response to Ka21 and Ka35. Permeabilities were allowed to differ for the two source wells.

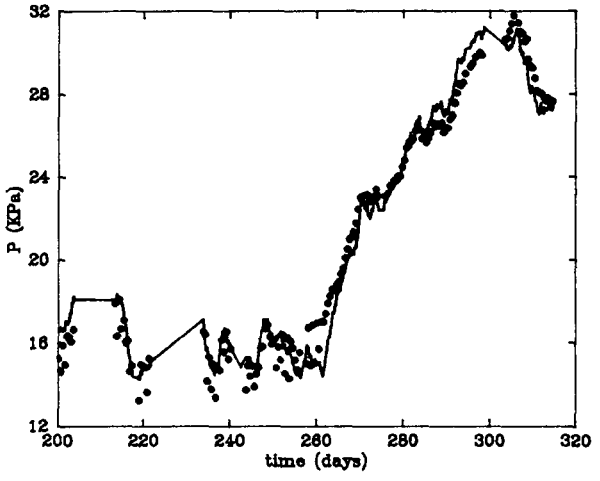

Figure 13: Ka14 pressure data and fitted finite reservoir with recharge response to Ka21 and Ka35. Permeabilities were allowed to differ for the two source wells. Response to Ka35 was insignificant.

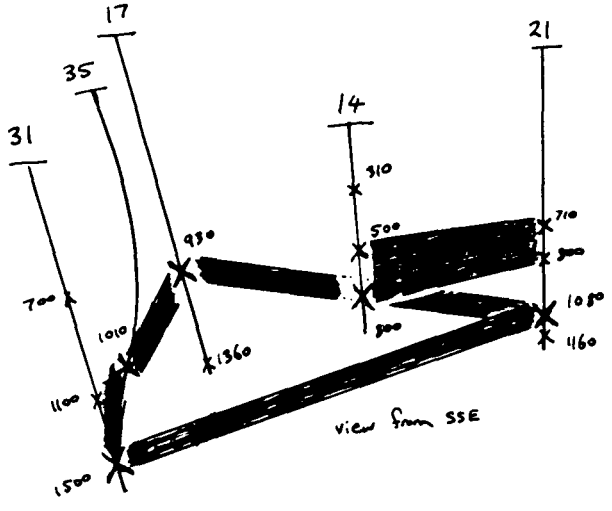

Figure 14: Possible communication paths of deep responding wells

3.1 Results

There is a consistent pattern in the fitted permeabilities in Table 2. The responses to Ka35 are smaller than those to Ka21, which gives larger permeabilities for Ka35 when using the infinite reservoir solution. This could be due to the existence of two deeper aquifers, one overlying the other. Ka21 with its multiple feedpoints may produce from both aquifers, affecting Ka14 pressures through its intermediate depth feedpoints and affecting Ka17 and Ka31 through its deepest feedpoints. See Figure 14 for a sketch of the possible communication paths.

The fitted permeabilities are high, consistent with a fractured reservoir.

The storativities ϕch are of comparable size to the values in Table 1, but with the compressibility of 260°C fluid, $c = 1.4 \times 10^{-9}\text{Pa}^{-1}$, reasonable values of ϕ result for Ka17 and Ka31. Ka14 has an anomalously high value, possibly reflecting communication with atmospheric pressure or two-phase fluid. Christenson (1986) associates degassing of fluid in the central part with a two-phase zone, surrounded by a region where the hot source fluid has mixed with cooler groundwaters.

The storage coefficients ϕcV obtained for these deep-feeding wells are larger than obtained for the shallow feeding wells, suggesting that there is more fluid available at deeper levels, about two or three times that available at shallow levels. If the values fitted to the early-time part of the solution are used, a reservoir volume of 120–140 Km^3 is obtained. With an assumed depth of 500 m, this implies an area of 240–280 Km^2, which is larger than expected at Kawerau.

The values obtained for the recharge coefficient mean that a 2 bar pressure drop would lead to 50–1400 Kg/s recharge flow. This compares with a total fluid mass production rate of up to about 400 Kg/s.

4 Conclusions

These interference tests conducted at Kawerau have led to new and vital insights into the reservoir's hydrological structure, which will point the way for improved numerical models.

Shallow feeding wells respond to injection into KaM3 in a manner consistent with a finite cylindrical reservoir model. These responses range over feed depths of about 85–400 m. There is no observable pressure communication between these wells and the deeper-feeding set of wells. The deeper-feeding wells communicate in a depth range of about 800–1010 m, in a manner consistent with a cylindrical reservoir model with lateral recharge.

A picture emerges of a smaller shallow reservoir overlying a larger deep reservoir. The shallow reservoir may be as large as 28–164 Km^2 in area. The deep reservoir may be up to 240–280 Km^2 in area. The shallow reservoir appears to be in communication with the atmosphere, and has small porosities, suggestive of the importance of fractures or contact planes. The deep reservoir has larger values of porosity, and some indication of possible communication with a two-phase zone. There is evidence of some structure in the deeper

reservoir, with larger pressure changes resulting from flow changes in Ka21 than Ka35.

This two-reservoir structure is confirmation of the good sense of the policy of drilling deeper wells at Kawerau. Shallow wells were short-lived presumably because of good communication with cooler overlying and surrounding groundwaters. Deeper wells are more shielded, by an umbrella possibly associated with sedimentary formations found at about 500 m depth in many petrological logs.

Acknowledgements

This work was made possible by the financial support of the Gas and Geothermal Trading Group, Ministry of Energy, Wellington, New Zealand. The tests were conducted and the data collected by the Ministry of Works and Development, Wairakei.

References

Burnell, J. G. and McGuinness, M. J. (1986) Kawerau Interference Tests (August–October 1985), an *Applied Mathematics Division Report* prepared for the Gas and Geothermal Trading Group, Ministry of Energy, Wellington, November 1986.

Christenson, B. W. (1986) Hydrology and Fluid Chemistry of the Kawerau Geothermal System, *in* The Kawerau Geothermal Field: Contributions from the 1982 Kawerau Seminar and Other Scientific Investigations, *DSIR Geothermal Report Number 10,* Chapter 5. This report was compiled for the Gas and Geothermal Trading Group, Ministry of Energy, New Zealand, and is confidential to them as a whole.

Gringarten, A. C. (1984) Interpretation of Tests in Fissured and Multilayered Reservoirs With Double-Porosity Behaviour: Theory and Practice, *J. Pet. Tech.* (April 1984) pp. 549–564.

Moench, A. F. (1984) Double Porosity Models for a Fissured Groundwater Reservoir With a Fracture Skin, *Water Resour. Res.* 20 #7 pp. 831–846.

McGuinness, M. J. (1985) Interference Between Ka17 and Ka27, *Report KA-1985-MJM-1* prepared for the Gas and Geothermal Trading Group, Ministry of Energy, Wellington.

McGuinness, M. J. (1986) Pressure Transmission in a Bounded Randomly Fractured Reservoir of Single-Phase Fluid, to appear in *Transport in Porous Media,* Volume 2.

Matthews, C. S. and Russell, D. G. (1967) *Pressure Buildup and Flow Tests in Wells,* Monogr. No. 1, SPE, Dallas, Texas.

Grant, M. A. (1985) Pressure Changes in the 500m Zone of Kawerau, *Report KA-1985-MAG-2,* prepared for the Ministry of Energy, Wellington.